SRTTU

JCARME
ISSN: 2228-7922

Journal of Computational and Applied Research
in Mechanical Engineering
Vol. 4, No. 2, pp. 121- 132, Spring 2015
http://jcarme.srttu.edu

Prediction of forming limit curves (FLD, MSFLD and FLSD) and necking time for SS304L sheet using finite element method and ductile fracture criteria

Kamal Kolasangiani [a,*], Mahmoud Shariati [a] and Khalil Farhangdoost [a]

[a] *Department of Mechanical Engineering, Ferdowsi University of Mashhad, Mashhad, Iran*

Article info:
Received: 16/03/2014
Accepted: 19/08/2014
Online: 03/03/2015

Keywords:
Forming limit curves,
Finite element method and ductile fracture criterion,
Necking time,
SS304L sheet,
Effect of thickness.

Abstract

Forming limit curves are used as a parameter in finite element analysis to control the material's level of formability. In this research, forming limit diagram (FLD) of SS304L sheet was obtained by ABAQUSfinite element software. In practice, the experimental determination of a forming limit curve is a very time-consuming procedure which requires special and expensive equipment. Forming limit diagram (FLD) is derived by the simulation of Erichsen test (out-of-plane stretching test) using hemispherical punch. There are few studies on the prediction of necking time, which is obtained by the application of Pepelnjak algorithm and ductile fracture criterion. In order for the validation, the numerical result of forming limit diagram (FLD) was compared with the experimental and analytical results and a good correlation was observed. Forming limit stress diagram (FLSD) and MSFLD were determined by plotting the principal in-plane stress and FLD corresponding to the onset of necking localization, respectively. Effect of the thickness of the sheet on forming limit curves was investigated and the results showed that increased thickness of the sheet led to raised level of the FLD and MSFLD; but, FLSD did not change considerably.

1. Introduction

Main mechanisms can cause the fracture of a ductile metal are necking, growth and coalescence of voids; and shear fracture due to shear band localization. Necking is main parameter in metal forming operation. The formability limit of sheet metal is obtained by the initiation of the local neck that leads to fracture. ABAQUSapplies four criteria for determining of formability limit of sheet metals: forming limit diagram (FLD); forming limit stress diagram (FLSD); Muschenborn-Sonne forming limit diagram (MSFLD); and Marciniak-Kuczynski (M-K) criteria.

The forming limit diagram (FLD) as an essential tool is applied to predict the onset of necking in sheet metal forming operations. Limit strains is the maximum strains which were in sheet metals before the onset of necking. A FLD is a plot of the forming limit strains in the space of principal (in-plane)

[*] *Corresponding author*
Email address: kamal.kolasangiani@gmail.com

strains. In the discussion that follows major and minor limit strains refer to the maximum and minimum values of the in-plane principal limit strains, respectively. The major limit strain is usually represented on the vertical axis and the minor strain on the horizontal axis, as illustrated in Fig. 1. The damage initiation criterion for the FLD is defined as the ratio of the current major principal strain at any elements, ε_{major}, to the major limit strain on the FLD evaluated at the current values of the minor principal strain, ε_{minor}. For example, for the deformation state given by point A in Fig. 1 the damage initiation criterion is evaluated as:

$$D=\frac{AH}{BH} \quad (1)$$

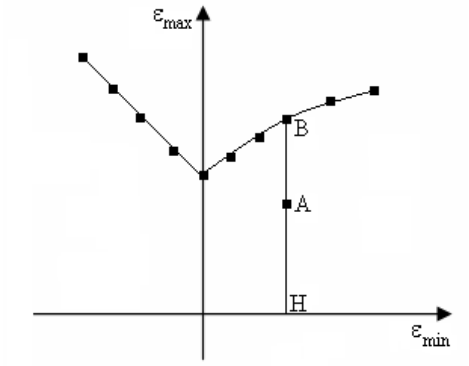

Fig. 1. Forming limit diagram (FLD).

Forming limit diagrams (FLDs) depend greatly on strain path. So, major changes are observed by converting the deformation mode (e.g. equibiaxial loading followed by uniaxial tensile strain). Therefore, the FLD damage does not have good performance when the strain path is nonlinear. In this condition, ABAQUSsoftware proposes two damage initiation criteria: forming limit stress diagram (FLSD) criterion, Muschenborn-Sonne forming limit diagram (MSFLD) criterion; using these criteria, the dependency of limit strains on load path is decreased.

An FLSD is the stress counterpart of the FLD, with the major and minor principal in-plane stresses corresponding to the onset of necking localization plotted on the vertical and horizontal axes, respectively. The damage initiation criterion for the FLSD is defined as the ratio of the current major principal stress, σ_{major}, to the major stress on the FLSD evaluated in the current values of minor stress, σ_{minor}.

Muschenborn and Sonne (1975) proposed a method for predicting the influence of the deformation path on the forming limits of sheet metals on the basis of the equivalent plastic strain, assuming that the forming limit curve represents the sum of the highest attainable equivalent plastic strains. The criterion of necking instability of sheet metals used in ABAQUSwas based on these assumptions for any deformation path. So, the Muschenborn-Sonne criterion changed the original forming limit curve (without pre-deformation effects) from the space of major versus minor strains to the space of equivalent plastic strain, $\bar{\varepsilon}^{pl}$, versus ratio of principal strain, $\alpha=\frac{\varepsilon_{minor}}{\varepsilon_{major}}$ (Fig. 2).

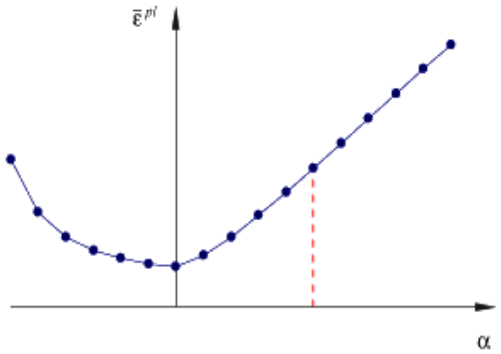

Fig. 2. Muschenborn-Sonne's forming limit diagram (MSFLD).

According to the MSFLD criterion, the onset of localized necking occurs when the sequence of deformation states in the $\bar{\varepsilon}^{pl}-\alpha$ diagram intersects the forming limit curve. It is shown that both FLD and MSFLD give identical results for linear deformation paths. But, for arbitrary loading, the MSFLD predicts the onset of necking by including the effects of the history of deformation as accumulated equivalent plastic strain. Necking instability also occurs if the sequence of deformation states in the $\bar{\varepsilon}^{pl}-\alpha$ diagram intersects the limit curve due to a sudden change in the straining direction. This situation is illustrated in Fig. 3.

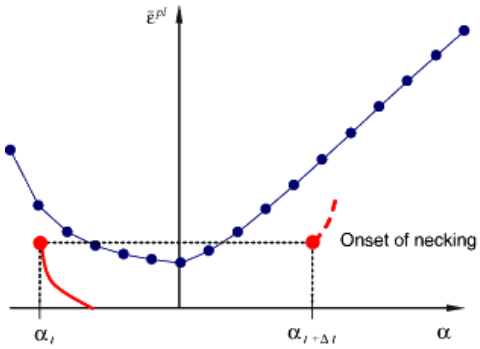

Fig. 3. Onset of necking by changing the straining direction in the MSFLD curve.

Several researchers have attempted to predict the forming limit diagrams, which was introduced by Keeler and Backofen (1964) for the first time to the fracture limits of sheet metals [1]. Wu et al. investigated the dependence of forming limit stress diagrams (FLSDs) on strain path and found that FLSD was independent from strain path [2]. Stoughton explained forming limit for both proportional and non-proportional loadings from a single criterion based on the stress state and validated it by the strain path history [3,4]. Stoughton and Zhu reviewed several theoretical models of sheet metal forming instability to change the strain space of FLD to stress space by assuming the isotropic hardening of yield surface [5]. Yoshida et al. studied the forming limit of aluminum AA5154-O tube under combined axial loads and internal pressure experimentally. They found that the path-dependence of forming limit curve vanished when translated into stress space [6]. Kuwabara et al. also presented the anisotropic plastic deformation behavior of aluminum alloy tubes by a servo-controlled testing machine under the isotropic hardening assumption for both linear and combined stress paths and observed that the isotropic hardening assumption was valid for both linear and combined stress paths [7]. Ahmadi et al. investigated the effect of work-hardening exponent and plastic strain ratio on forming limit diagrams (FLDs). They concluded that, by increasing the value of work-hardening exponent, values of FLD were increased [8]. Ganjiani and Assempour focused on the prediction of the forming limit diagram based on the M-K theory. The results were compared with the experimental data in other papers [9]. Assempour et al. studied the effect of strain path on the shape and level of FLSD by applying the M-K model and showed that the FLD was more sensitive to the strain path effect than FLSD [10]. Dariani et al. investigated the effect of forming speed on the formability of 6061-T6 aluminum alloy and AISI 1045 steel sheet, both numerically and experimentally. They found considerable results in formability at high velocity forming from experimental data [11]. Assempour et al. examined the normal stress on formability sheet metal. So, they found FLD based on M-K model by modifying the stress state and observed that the compressive normal stress became higher in FLD [12]. Hashemi and Abrinia studied the effect of through-thickness normal stress on the extended stress-based FLC [13]. Mamusi et al. presented a novel numerical method by three necking criteria to predict the FLDs of Tailor-Welded blanks. All three criteria had identical results [14]. Panich et al. presented experimental and numerical analyses of forming limit diagram (FLD) and forming limit stress diagram (FLSD) for two advanced high strength steel (AHSS) sheets, grade DP780 and TRIP780. There was a correlation between analytical calculations and experimental results; the stress-based forming limit curves were more accurate than the strain-based forming limit curves [15].

Pepelnjak et al. presented a method for calculating the FLD using numerical simulation by ABAQUSprogram. They predicted the FLD using Marciniak testing procedure and determined the critical areas, in which the onset of necking occurred. The thickness strain, first and second derivation of thickness strain, was also analyzed as a function of time for these areas [16].

Ozturk and Lee predicted the forming limit diagram (FLD) of sheet metal by applying ductile fracture criteria and comparison with experimental and analytical curves [17]. Takuda et al. focused on limit strains in the biaxial stretching of aluminum alloy sheets by combining the finite element simulation and ductile fracture criterion for various strain paths. They observed s good agreement

between numerical results and experimental data [18].
According to the above research, few studies have investigated and predicted necking time using ductile fracture criteria. In this paper, necking time was predicted by ductile fracture criteria in ABAQUSsoftware and then forming limit curves (FLD, FLSD, MSFLD) of steel 304L were determined. The experimental and analytical results by Ozturk and Lee [17] were used to confirm the validity of the numerical method.

2. Ductile fracture criterion

The purpose of this study was to predict the necking time by combining finite element simulation with ductile fracture criteria. So, the necking time can be predicted by substituting stress and strain values by the ductile fracture criteria. Some criteria have been proposed to show the effect of deformation history.
Cockcroft and Latham [19] proposed a fracture criterion for ductile material. , based on which, the fracture occurred when

$$\int_0^{\bar{\varepsilon}_f} \sigma_{max} d\bar{\varepsilon} = C_1 \quad (2)$$

where σ_{max} is maximum normal stress, $\bar{\varepsilon}_f$ is fracture strain, and C_1 is material constant. Brozzo et al. [20] modified Cockcroft and Latham's criterion by considering the effect of hydrostatic stress, σ_h, to accurately predict the fracture of sheet metal.

$$\int_0^{\bar{\varepsilon}_f} \frac{2\sigma_{max}}{3(\sigma_{max}-\sigma_h)} d\bar{\varepsilon} = C_2 \quad (3)$$

C_2 is material constant. Clift et al. [21] proposed a fracture criterion based on energy criteria or plastic work as follows:

$$\int_0^{\bar{\varepsilon}_f} \bar{\sigma}\, d\bar{\varepsilon} = C_3 \quad (4)$$

where $\bar{\sigma}$ and C_3 are equivalent stress and material constant, respectively. The equivalent strain and equivalent stress can be introduced by assuming plastic incompressibility and neglecting elastic strain in Eq. (5) and Eq. (6).

$$\bar{\varepsilon} = \sqrt{\frac{4}{3}(1+\alpha+\alpha^2)}\varepsilon_1 \quad (5)$$

$$\bar{\sigma} = k\bar{\varepsilon}^n \quad (6)$$

3. Numerical analysis

In this research, simulations of Erichsen test were carried out using the general finite element ABAQUSprogram for specifying forming limit curves.

3. 1. Geometry and mechanical properties of the shells

The sheets used in this work were SS304L with two thicknesses (t=0.81 and 1.4mm). The specimens with different dimensions were used within the same tooling for forming, as shown in Figs. 4 and 5.
To determine the mechanical properties of sheets, simple tension test was performed according to ASTME8 standard test [23] by a servo hydraulic INSTRON 8802 machine (Fig. 6). The obtained results are shown in Fig. 7. In this study, the isotropy was considered and the von Misses yield criterion is used. The yield stress of SS304L was determined by drawing 0.2% line. Strain hardening coefficient (n) and strength coefficient (k) at $\sigma=k\varepsilon^n$ were by plotting $\log\sigma$-$\log\varepsilon$. Table 1 shows the mechanical properties of SS304L obtained from the experimental tests.
Plastic strain can be specified by Eq. (7).

$$\varepsilon_{pl} = \varepsilon_{real} - \frac{\sigma_{real}}{E} \quad (7)$$

The material constants of ductile fracture criterion were evaluated by stress-strain curve obtained from tension test. For tension test, the values of Cockroft and Latham, Brozzo et al, and Clift et al. were calculated by substituting $\sigma_{max}=\sigma_1$, $\sigma_h=\frac{\sigma_1}{3}$; these values were equal to C_1, C_2, and C_3, respectively. In this research, the values of C_1, C_2, and C_3 were 309.104, 0.37, and 315.96 MPa, respectively.

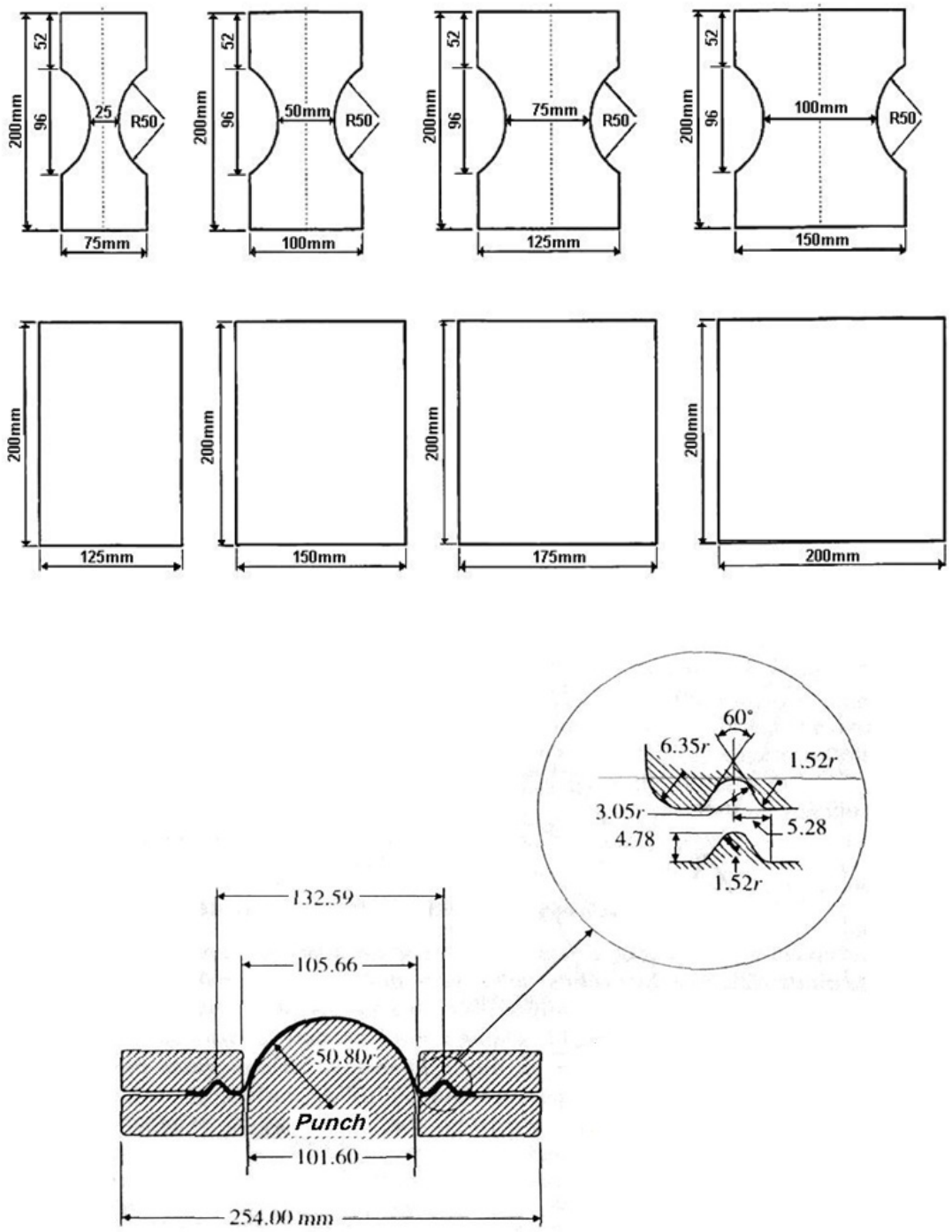

Fig. 5. Out-of-plane stretching test (Erichsen test) [22].

Fig. 6. Tension test by a servo hydraulic INSTRON 8802 machine.

3. 2. Element formulation of sheet

For this analysis, the nonlinear element S4R, which is a four-node element, was used. For the sake of symmetry, half of the specimen was modeled and, as moving from the edge to the sheet center, size of the element became smaller (Fig. 8).

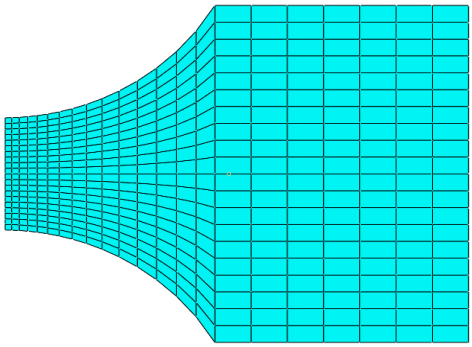

Fig. 8. A sample of FEM mesh.

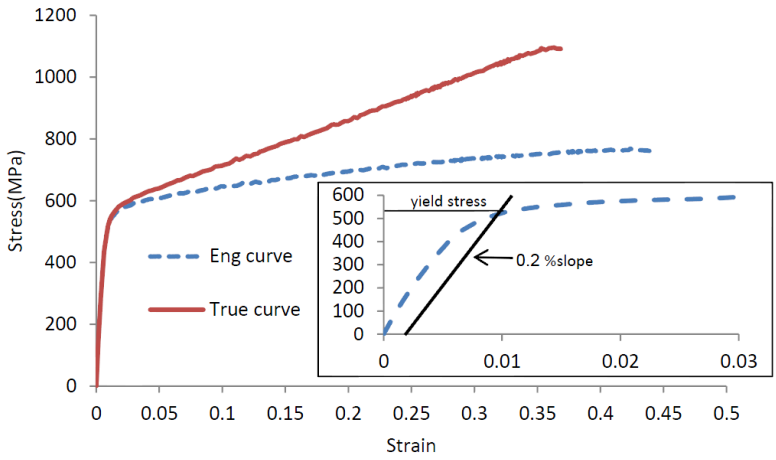

Fig. 7. Stress-strain curve of tension test for SS304L specimen.

Table 1. Mechanical properties of SS304L.

Modulus elasticity (GPa)	Yield stress (MPa)	Ultimate stress (MPa)	Poisson's ratio	Strain hardening coefficient	strength coefficient (MPa)	density (kg/m^3)
202.495	513.01	768.41	0.3	0.213	1277.909	7833

3. 3. Loading and boundary conditions

Loading is applied in two steps. In the first step, punch, sheet, and lower rigid die are fixed and blankholder moves down and deforms the sheet into the drawbead to prevent surfaces from slipping. The sheet is completely adhered to the blanholder and die. In the next step, rigid die, sheet, and blankholder stay fixed and the punch starts to move up until the given displacements are achieved. The punch
moves up to deform the sheet at the speed of 50 mm/min.

3. 4. Contact

The surface-to-surface contact formulations are considered for this case. Interaction defines the die and balnkholder as the master surface with sheet as the slave surface. In addition, penalty contact formulation is tested to permit
some relative motion of the surfaces (an elastic slip) with the fiction coefficient of 0.16.

3. 5. Analytical process

In this research, a dynamic simulation was used and necking time was obtained by applying Pepelnjak algorithm [16] based on Marciniak-Kuzinsky method. The presented paper introduced the methodology of spatial identification of the necking of critical nodes of the FEM model and determined their corresponding maximum and minimum strains. The nodes with minimal thickness were selected to obtain their thinning as a function of forming simulation time. First and second derivations of thinning for the selected nodes were calculated. The node at which the maximum of the second derivation of thinning first appeared (at minimal time) was assumed as the critical node where the onset of necking started. For example, the thinning along with the first and second derivation of thinning of sample 7, at critical node as a function of time is shown in Fig. 9. The location of the critical node of sheet metal is given in Fig. 10.
In order to determine the accurate time of necking using ductile fracture criteria, the values of ductile fracture criteria (D) were computed, as shown in Figs. 11-13. Necking occurred when the values of ductile fracture criteria were higher than the one determined from tensile test. Necking line position was at the point where the value of ductile fracture criteria was equal to the material constant obtained from tension test. So, according to Figs. 11-13, the value of ductile fracture criteria increased with increasing time to the moment that a point was placed on the upper necking line for first time. At this time, necking occurred.

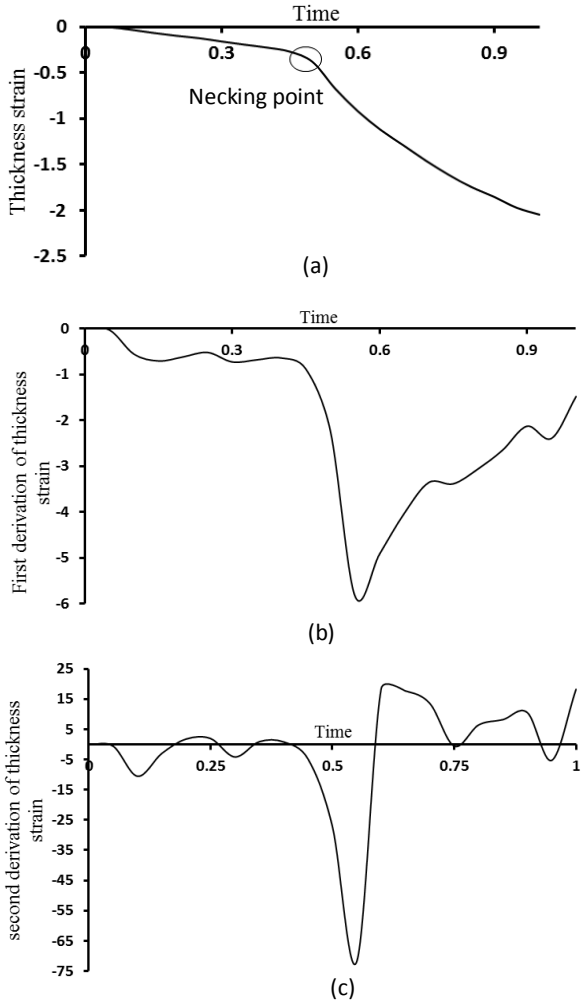

Fig. 9. a) Thickness strain as a function of time, b) First derivation of thickness strain as a function of time, c) Second derivation of thickness strain as a function of time.

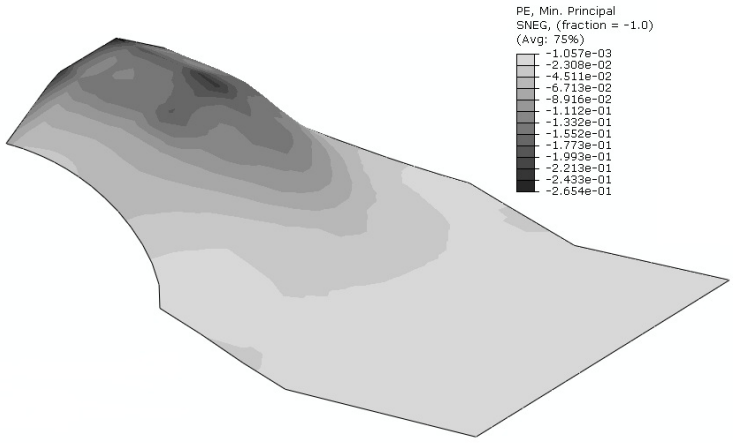

Fig. 10. Minimum principal strain contour of sheet in Abaqus.

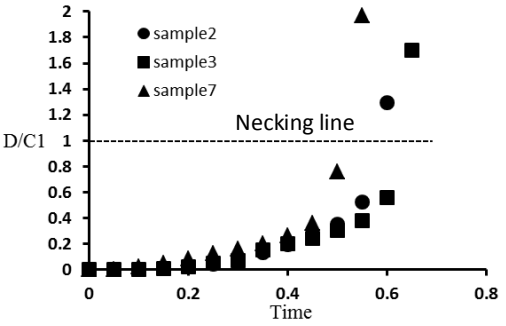

Fig. 11. Values of Cockroft and Latham's criterion versus time at critical node.

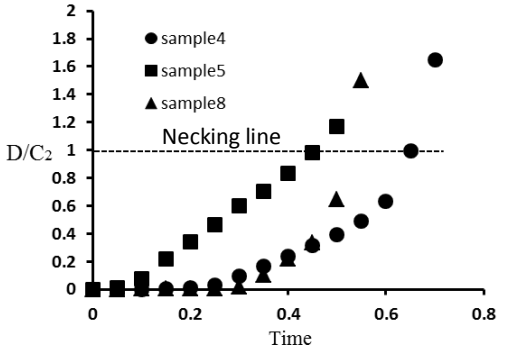

Fig. 12. Values of Brozzo et al.'s criteria versus time at critical node.

The necking times based on the ductile fracture criteria were computed for the time period of 1 second and listed in Table 2. There was good correlation between the times of necking for different ductile fracture criteria.

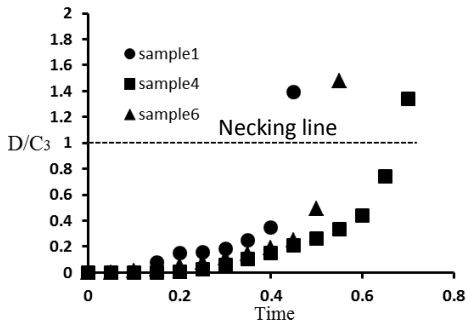

Fig. 13. Values of Clift et al.'s criteria versus time at critical node.

4. Confirming numerical results by experimental and analytical data

In order for the validation, the numerical results were compared with the experimental and analytical results proposed by Ozturk and Lee [17]. The material properties of sheet metal in [17] are summarized in Table 3. FLD of the numerical results was compared with the experimental and analytical results in Fig. 14. The numerical data at the left side of the FLD predicted larger maximum strain than the experimental results; but, they were very close to the analytical curve. Shape of
the curve on the right side of the FLD was in accordance to the experimental curve.

5. Results of numerical analysis

The limit strains were determined by selecting critical node and specifying necking time for all the samples. Forming limit diagram (FLD) of SS304L sheet metal is shown in Fig. 15. The onset of the localized necking occurred when the strain state intersected the forming limit diagram.

FLSD curve, by plotting the major principal in-plane stress versus the minor principal-in plane stress at necking time for all the samples, is shown in Fig. 16. Also, according to Fig. 17, the MSFLD curve represented the equivalent plastic strain from Eq. (5) versus ratio of principal strain at the damage initiation of SS304L sheet metal for all the samples. As said in the previous sections, the MSFLD representation took into account of the effects of the history of deformation through the use of the accumulated equivalent plastic strain.

The M-K criterion can accurately capture the effects of nonlinear strain paths; however, it is computationally expensive, especially if large numbers of imperfection orientations are introduced. It has been verified that the results obtained by the MSFLD criterion are similar to those obtained using the M-K criterion, but with much reduced computational expense.

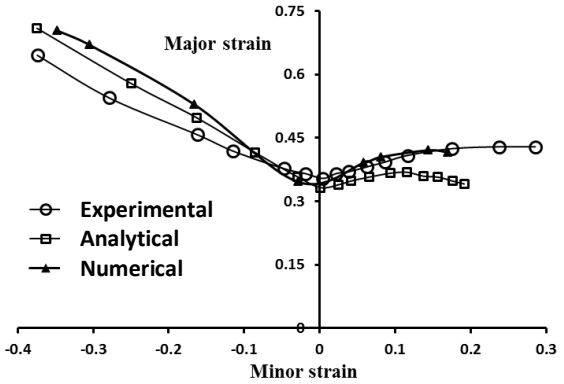

Fig. 14. Comparing numerical results with the results proposed by Ozturk and Lee [17].

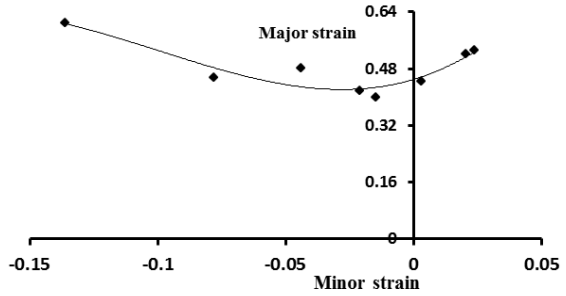

Fig. 15. FLD curve of SS304L sheet metal with 0.81mm thickness.

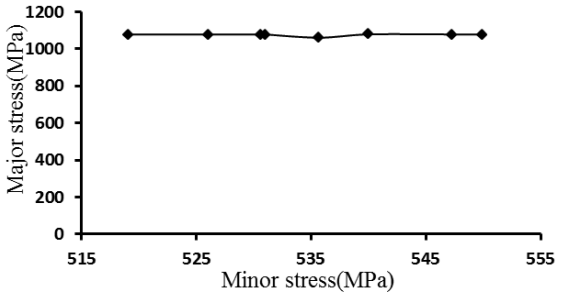

Fig. 16. FLSD curve of SS304L sheet metal with 0.81mm thickness.

5. 1. Effect of shell thickness on FLD, FLSD, and MSFLD

In this section, sheet metal of SS304L with 0.81 and 1.4mm thickness was simulated in Abaqus. Some papers have shown the considerable effect of thickness on the sheet formability [24]; others have said that the FLDs differ slightly if micro-structure does not vary by changing thickness in the manufacturing process [25]. As mentioned in [24], for thin sheets, there is no significant difference in FLD by varying thickness; but, it is not true for thick sheets. As shown in Figs. 18-19, when the sheet thickness increased, the FLD and MSFLD curves were placed at a higher level; so, formability was improved. But, according to Fig. 20, increasing the shell thickness was not effective for the FLSD curve. Generally, the limit strains were sensitive to thickness, whereas the limit stresses were not.

Table 2. Necking time based on ductile fracture criteria at critical node.

Number of sample	1	2	3	4	5	6	7	8
Necking time based on Cockroft and Latham criteria	0.45	0.6	0.65	0.7	0.55	0.55	0.55	0.55
Necking time based on Brozzo et al. criteria	0.45	0.6	0.65	0.7	0.5	0.55	0.55	0.55
Necking time based on Clift et al. criteria	0.45	0.6	0.65	0.7	0.55	0.55	0.55	0.55

Table 3. Mechanical properties of sheet metal in [17].

Modulus elasticity (GPa)	Yield stress (Mpa)	Ultimate stress (MPa)	Poisson'ratio	Strain hardening coefficient	strength coefficient (MPa)	density (kg/m^3)
200	174	288.33	0.3	0.202	480.43	7833

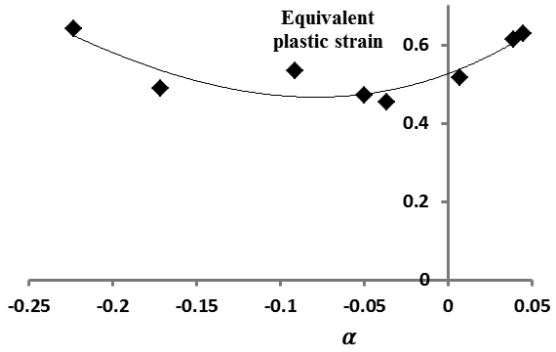

Fig. 17. MSFLD curve of SS304L sheet metal with 0.81mm thickness.

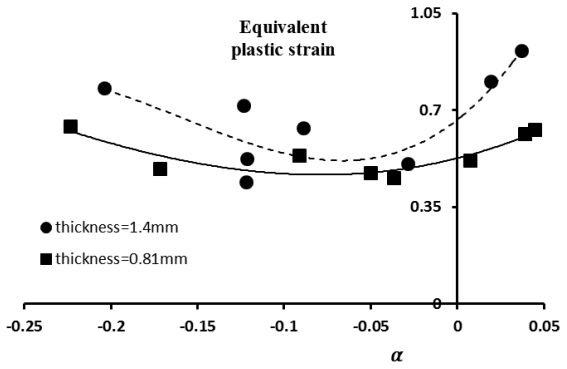

Fig. 19. MSFLD curve of SS304L sheet metal with two thicknesses.

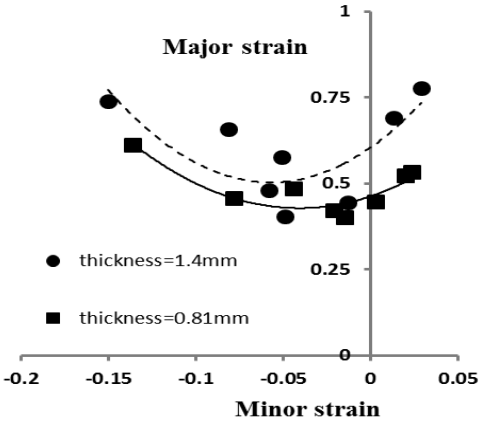

Fig. 18. FLD curve of SS304L sheet metal with two thicknesses.

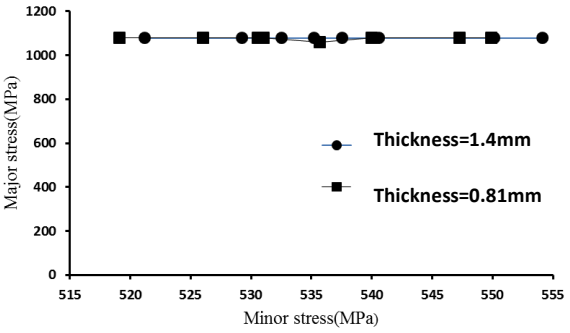

Fig. 20. FLSD curve of SS304L sheet metal with two thicknesses.

6. Conclusions

In this paper, Erichsen test (out-of-plane stretching test) of SS304L sheet metal was simulated by ABAQUSsoftware. Based on the results, the following conclusions were made:

- According to Pepelnjak algorithm, localized necking time was determined by obtaining thinning or thickness deformation as a function of time and calculating the first and second derivations of thinning for critical node. Due to the fast local change of sheet thickness at the necking point, the thickness strain leaping changed its value. Also, based on ductile fracture criteria, the value of ductile fracture criteria increased with increasing time and necking occurred when the value of ductile fracture criteria was larger than the one obtained from tension test. The prediction time of necking for three ductile fracture criteria was fairly the same. Also, there was a good agreement between necking times; the ones determined by applying ductile fracture criteria and the one evaluated by Pepelnjak algorithm.
- The forming limit diagram (FLD) of finite element ABAQUSsoftware was compared with the experimental and analytical results. On the left side of the FLD, the numerical results were closer to the analytical data, while on the right side, the results of simulation were in agreement with the experimental data. Generally, the difference between numerical, experimental, and analytical results was not significantly large.
- Level of the FLD and MSFLD curve increased with increasing sheet thickness, whereas there was no change in the FLSD curve. So, by changing the sheet thickness, the maximum limit strains were increased considerably; but, the limit stresses were not sensitive to the variation of sheet thickness.

References

[1] S. P. Keeler and W. A. Backhofen, "Plastic instability and fracture in sheet stretched over rigid punches", *ASM Transactions Quarterly*. Vol. 56, No. 11, pp. 25-48, (1964).

[2] P. D. Wu, A. Graf, S. R. MacEwen, D. J. Lloyd, M. Jain and K. W. Neale, "On forming limit stress diagram analysis", *Int. J. of Solids and Structures*. Vol. 42, No. 8, pp. 2225-2241, (2005).

[3] T. B. Stoughton, "A general forming limit criterion for sheet metal forming", *J. Mech. Sci.* Vol. 42, No. 1, pp. 1-27, (2000).

[4] T. B. Stoughton, "Stress-based forming limits in sheet-metal forming", *ASME J. Eng. Mater. Technol*. Vol. 123, No. 4, pp. 417-422, (2001).

[5] T. B. Stoughton and X. Zhu, "Review of theoretical models of the strain-based FLD and their relevance to the stress-based FLD", *Int. J. Plast.* Vol. 20, No. 8-9, pp. 1463-1486, (2004).

[6] K. Yoshida, T. Kuwabara, K. Narihara and S. Takahashi, "Experimental verification of the path independence of forming limit stresses", *Int. J. Form. Processes*. Vol. 8, No. 1, pp. 283-298, (2005).

[7] T. Kuwabara, K. Yoshida, K. Narihara and S. Takahashi, "Anisotropic plastic deformation of extruded aluminum alloy tube under axial forces and internal pressure", *Int. J. Plast.* Vol. 21, No. 1, pp. 101-117, (2005).

[8] S. Ahmadi, A. R. Eivani and A. Akbarzadeh, "Experimental and analytical studies on the prediction of forming limit diagrams", *Comput. Mater. Sci.,* Vol. 44, No. 4, pp. 1252-1257, (2009).

[9] M. Ganjiani and A. Assempour, "An improved analytical approach for determination of forming limit diagrams considering the effects of yield functions", *J. Mater. Process. Technol.,* Vol. 182, No. 1-3, pp. 598-607, (2007).

[10] A. Assempour, R. Hashemi, K. Abrinia, M. Ganjiani and E. Masoumi, "A methodology for prediction of forming limit stress diagrams considering the strain path effect", *Comput. Mater. Sci.,* Vol. 45, No. 2, pp. 195-204, (2009).

[11] B. M. Dariani, G. H. Liaghat and M. Gerdooei, "Experimental investigation of sheet metal formability under various strain rates", *Proceedings of the Institution of Mechanical Engineers, Part B: Journal of Engineering Manufacture,* Vol. 223, No. 6, pp. 703-712, (2009).

[12] A. Assempour, H. K. Nejadkhaki and R. Hashemi, "Forming limit diagrams with the existence of through-thickness normal stress", *Comput. Mater. Sci.,* Vol. 48, No. 3, pp. 504-508, (2010).

[13] H. Mamusi, A. Masoumi, R. Hashemi and R. Mahdavinejad, "A novel approach to the determination of forming limit diagrams for tailor-welded blanks", *J. Mater. Eng. Perform.,* Vol. 22, No. 11, pp. 3210-3221, (2013).

[14] R. Hashemi and K. Abrinia, "Analysis of the extended stress-based forming limit curve considering the effects of strain path and through-thickness normal stress", *Mater. Des.,* Vol. 54, No. 1, pp. 670-677, (2014).

[15] S. Panich, F. Barlat, V. Uthaisangsuk, S. Suranuntchai and S. Jirathearanat, "Experimental and theoretical formability analysis usingstrain and stress based forming limit diagram for advanced high strength steels", *Mater Des*. Vol. 51, No. 1, pp. 756-66, (2013).

[16] T. Pepelnjak, A. Petek and K. Kuzman, "Analysis of the Forming Limit Diagram in Digital Environment", *Adv. Mater. Research.,* Vol. 6-8, No. 1, pp. 697-704, (1972).

[17] F. Ozturk and D. Lee, "Analysis of forming limits using ductile fracture criteria", *J. of Mater. Process. Tech.,* Vol. 147, No. 3, pp. 397-404, (2004).

[18] H. Takuda, K. Mori, N. Takakura and K. Yamaguchi, "Finite element analysis of limit strains in biaxial stretching of sheet metals allowing for ductile fracture", *Int. J. Mech. Sci.,* Vol. 42, No. 4, pp. 785-798, (2000).

[19] M. G. Cockroft and D. J. Latham, "Ductility and the Workability of Metals", *J.Inst. Met.,* Vol. 96, No. 2, pp. 33-39, (1968).

[20] P. Brozzo, B. Deluca and R. Rendina, "A New Method for the Prediction of Formability in Metal Sheets", *In: Proceedings of the 12th Biennial Congress of the IDDRG, on Sheet Metal Forming and Formability*, (1972).

[21] S. E. Clift, P. Hartley, C. E. N. Sturgess and G. W. Rowe, "Fracture Prediction in Plastic Deformation Processes", *Int. J. Mech. Sci.* Vol. 32, No. 1, pp. 1-17, (1990).

[22] S. Kalpakjian and S. R. Schmid, "Sheet Metal Forming Process", *Prentice-Hall, 4th Edition*, (2000).

[23] ASTM A370-05 "Standard test methods and definitions for mechanical testing of steel products".

[24] S. A. Jenabali jahromi, A. Nazarboland, E. Mansouri and S. Abbasi, "Investigation of formability of low carbon steel sheets by forming limit diagrams", *Iranian Journal of Science & Technology, Transaction B, Engineering,* Vol. 30, No. B3, pp. 377-385, (2006).

[25] R. Hashemi, A. Ghazanfari, K. Abrinia, and A. Assempour "Forming limit diagrams of ground St14 steel sheets with different thicknesses", *SAE International Journal of Materials & Manufacturing,* Vol. 5, No. 1, pp. 60-64, (2012).